Statistical Inference of Cloud Thickness from NOAA 4 Scanning Radiometer Data

WILLIAM JOHN KAVENEY, ROBERT G. FEDDES AND KUO-NAN LIOU

Department of Meteorology, University of Utah, Salt Lake City 84112

(Manuscript received 20 June 1976, in revised form 11 October 1976)

ABSTRACT

A statistical correlation between cloud thickness and brightness is shown by regression analyses using the least-square method. Cloud thicknesses are obtained from two sources; pilot reports and the three-dimensional nephanalysis program (3DNEPH) for cases of single stratus and stratocumulus layers. Brightness values are obtained from the NOAA 4 satellite scanning radiometer. Regression analyses are performed on both thickness data sources used in conjunction with the scanning radiometer data. The results are shown by the regression curve relating pilot report thicknesses and brightness accounting for 66% of the variance in the cloud thickness, and the regression curve relating 3DNEPH thicknesses and brightness accounting for 46% of the variance in the cloud thickness. Moreover, in view of the effect of cloud compositions on the cloud brightness, regression analyses are performed on both thickness data sources excluding those cases whose origin is an unstable maritime tropical air mass. Results of these regression analyses reveal increases in the correlation between cloud thickness and brightness with 88% and 55% of the variances accounted for by pilot reports and 3DNEPH program data sources, respectively.

1. Introduction

Since the advent of operational weather satellites, meteorologists have sought new and improved ways of exploiting the tremendous amounts of data available through this new medium for the inference of the cloud structure and composition in the earth's atmosphere. Recently, the work of Park *et al.* (1974) has shown a statistical relationship between the thickness of cumulonimbus clouds and their reflected solar radiance (brightness). However, the approach which was taken in their study to achieve the statistical correlation between cloud thickness and brightness seems to be hampered by a number of misleading assumptions made in the statistical analysis. For example, the clouds used in the study were considered to be blackbodies; however, it is not obvious how a blackbody cloud and a cloud with a lesser emissivity could be distinguished using satellite radiance measurements. Because one cannot easily correct for the different emissivities of clouds, appreciable errors in the evaluation of the cloud-top temperatures used in the study could be introduced. In addition, the relationship between cloud brightness and the cloud-top temperature, one of the basic premises of the study, is not easily understood since the brightness of a cloud is determined by composition and thickness, and not by its position in the atmosphere as is implied by the cloud-top temperature. Because of these shortcomings, as well as others discussed by Gruber (1975) and Liou (1975), an alternate method was taken to arrive at a statistical relationship between cloud thickness and brightness directly.

The hypothesis that cloud thicknesses can be inferred from brightness values has a physical basis. Clouds of different thicknesses have different radiative transmission properties, that is, optically thick clouds will transmit less solar radiation than those of less thickness. Consequently, the less solar radiation in the visible part of the spectrum that is transmitted and absorbed, the more solar radiation will be reflected and the higher the brightness value will be. In addition to the cloud thickness, the physical properties of clouds, such as liquid water content (LWC) and drop size distribution (DSD) will also affect the radiative transmission properties of those clouds (see, e.g., Liou, 1976; Twomey, 1976). For example, if two clouds of equal thickness had appreciable differences in liquid water content and drop size distributions, the cloud with the greater LWC and the larger DSD would transmit less radiation than the other.

The objective of this study is to show a statistical relationship between cloud thickness and brightness, as observed from the NOAA 4 satellite, for low-level cloud decks which have no middle or high clouds present. Cloud thicknesses are obtained from two sources; pilot report data and the Air Force Global Weather Central three-dimensional nephanalysis program (3DNEPH). Thus, two independent sets of data are formed. Brightness values are obtained from the scanning radiometer of the NOAA 4 satellite. Owing to the effect of cloud compositions on cloud brightness

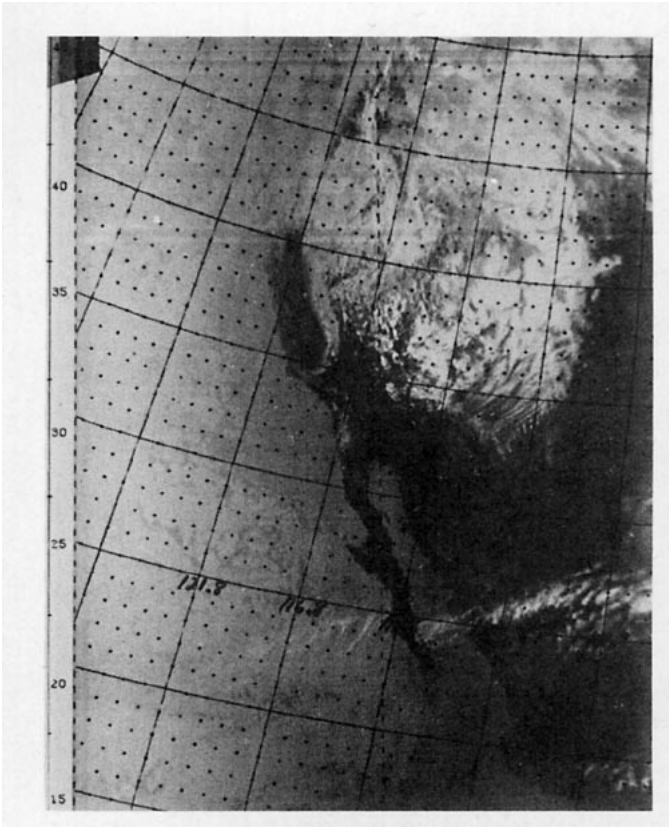

FIG. 1. 5 May 1975 DMSP IR satellite picture with pass time 1920 GMT.

values mentioned in the previous paragraph, the simple concept of air mass origin for clouds is employed in statistical analyses. Since clouds of tropical (or maritime) origin are normally unstable, that is, the particle size and size spectrum change rapidly within the cloud, one could anticipate that clouds of polar (or continental) origin would give a better correlation between the cloud thickness and brightness.

In order to find a statistical relationship between cloud thickness and brightness, the least-squares method is used to fit the pilot report data and the 3DNEPH data to regression curves. A coefficient of determination is then found for each of these curves. These coefficients of determination are finally tested for statistical significance using a t test. Similarly, two other regression curves are found to fit the thicknesses of aircraft reported clouds and the 3DNEPH derived clouds whose air mass origin is different from maritime tropical. Coefficients of determination are also derived from these curves.

A description of how pilot reports were chosen and the synoptic weather pattern involved with each pilot report are presented in Section 2. In Section 3 the NOAA 4 satellite and its scanning radiometer package are described, as well as the way in which brightness values were obtained. Section 4 describes the three-dimensional nephanalysis program, the criteria used for the selection of cases, and the general weather pattern involved with these cases. Finally, a description of the regression analyses used to correlate cloud thickness and brightness, are contained in Section 5. General conclusions are cited in the last section.

2. Pilot report selection

Pilot reports (PIREPS) were gathered for 5 May and 11 October 1975 over the continental United States. These pilot reports were then screened for their applicability to this study. The following are criteria for the rejection of a pilot report's applicability: 1) multilayered clouds were reported; 2) the reported cloud deck was not stratus or stratocumulus; 3) the reported cloud deck was not overcast or at least broken. The remaining pilot reports were compared to the general surface and upper air synoptic conditions, as well as surface observations near the reported area. This was done to check both the accuracy and applicability of the PIREP. Remarks attached to the PIREP, such as "clear above," were not questioned; however, surface observations were still consulted for any observation of cirriform clouds if the PIREP was taken at a time other than the time of NOAA 4 pass. If surface observations indicate cirrus, the PIREP was discarded.

Additional PIREP screening was made by verifying them with surface observations. In the case when

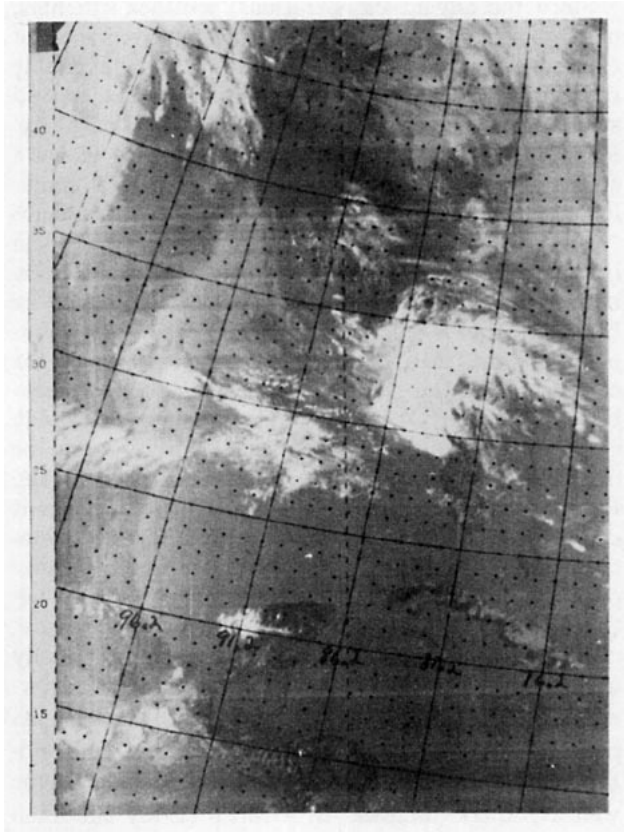

FIG. 2. As in Fig. 1 except pass time 1735 GMT.

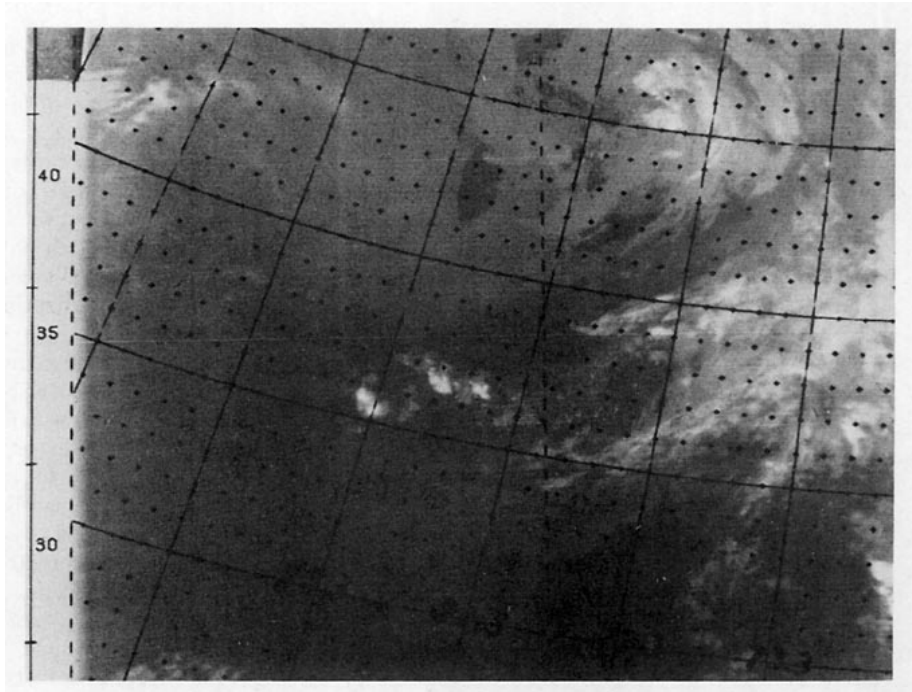

FIG. 3. 11 October 1975 DMSP IR satellite picture with pass time 1157 GMT.

only the cloud top was reported, the cloud thickness was obtained by determining the cloud base from the nearest reporting station and converting this base report to mean sea level and thus obtain a cloud thickness.

To corroborate the PIREPS and verify the presence of stratus clouds, Defense Meteorological Satellite Program (DMSP) infrared pictures were obtained from the University of Wisconsin for the two days in the study. The resolution of these pictures is 2 n mi and the gridding accuracy is $\pm 0.2°$ along the subtrack. Fig. 1, having a nodal crossing time of 1920,[1] shows the western third of the United States. Of interest in this picture is the upper level closed low-pressure center which is located at approximately 42°N, 113°W. Relatively low cloud-top heights, determined from the grey scale of the picture, are evident in western Washington, Oregon, and northern California. Fig. 2, having a nodal crossing time of 1735, shows the eastern two-thirds of the United States. It is evident from the grey shades of the picture that a low cloud deck extended from approximately 39.5° to 28°N. This cloud deck had imbedded cumulonimbus at about 30.5°N, 97.7°W. Low clouds were also evident over the Great Lakes and in the area of 41°N, 78°W.

Only one DMSP IR satellite picture was available for 11 October. Fig. 3 shows this IR picture covering the north-central United States at a nodal crossing time of 1157. The circulation of a closed low-pressure area can be seen in the Great Lakes area with the center of the low at approximately 45°N, 85°W. From the grey scales of the picture, relatively low cloud tops are evident in the Lake Superior, northern Lake Michigan, Lake Huron, and southern Lake Erie area. A weak frontal system is also shown across the center of the picture from 35°N, 88°W to 78°W and intensification is evident from the dense high clouds further to the northeast.

Since there was no DMSP coverage for the western United States on 11 October, brief descriptions of the synoptic situation are presented. At 1200 GMT the area of the United States west of the Rocky Mountains was under the influence of low pressure, which at 500 mb was centered along the Oregon and California border. The trough axis extended across northern California southwestward into the Pacific Ocean. The surface low was centered in east-central Nevada and had a cold front extending across central Nevada, southern California and southwestward into the Pacific Ocean. The central, southern and southeastern United States were all under high pressure. The 500 mb ridge was oriented northwest–southwest across the plains states, and the southeastern United States was under the influence of the Bermuda high centered in the Gulf of Mexico.

Errors in the calculated cloud thickness are from two sources. The first error is mainly attributed to the judgment of the pilot and the inherent error of the altimeter instrument. This could produce a total error by as much as 150 ft in the thickness determination. The second possible error may be from PIREPS with cloud-top information only when the cloud base is

[1] All times are GMT.

TABLE 1. Conversion of coded values to footlamberts and temperature (K) in visible and IR data, respectively.

Brightness		IR	
Footlamberts*	Coded value	Temperature (K)	Coded value
0–39	0	164.0	0
40–79	1	165.0	1
80–119	2	⋮	⋮
⋮	⋮	242.0	78
⋮	⋮	242.5	79
⋮	⋮	243.0	80
10160–10199	254	⋮	⋮
Missing data	255	330.0	254
		Missing data	255

* A unit of brightness (or luminance) equal to $(1/\pi)$ candles ft^{-2}.

determined from the surface observation. Care was taken for cases involving mountainous terrain to avoid the over- or underestimation of the cloud thickness.

3. NOAA 4 scanning radiometer data

a. Satellite and sensor description

Visual and infrared scanning radiometer data from the NOAA 4 satellite was obtained from the National Environmental Satellite Service (NESS) for 5 May and 11 October 1975. The NOAA 4 satellite is in a nominal 732 n mi orbit and has a period of 115 min. The satellite has a 78° inclination in a retrograde orbit thus providing a sun synchronous nodal crossing with the equator at approximately 0850 and 2050 LST. The scanning radiometer package on the NOAA 4 satellite contains a visual channel in the 0.52–0.73 μm range and an infrared channel in the 10.5–12.5 μm range.

The scanning radiometer sensor is spin stabilized having a rotating flywheel which spins perpendicularly to the orbital track and counter to the spin of the radiometer so that the sensor rotates only once per orbit. The sensor is earth oriented by use of pitch sensors, which regulate the speed of the flywheel with respect to the speed of the satellite in its orbital path, and attitude controls, which are provided by on board coils providing the needed magnetic torquing. The resolution of this scanning radiometer is approximately 2 n mi in the visible region and 4 n mi in the infrared near the satellite subpoint. Because of its orbit, the NOAA 4 satellite provides three sets of data of global coverage per day—two in the infrared and one in the visible range.

Additional information concerning the NOAA 4 satellite and its scanning radiometer package can be found in reports by Conlan (1973) and Schwalb (1972).

b. Characteristics of scanning radiometer data

As described in a report by Conlan (1973) there are three important factors concerning the scanning radiometer which must be considered before any of its data can be used in this study. The first of these is the calibration and sun normalization of visible data.

Prior to the launch of the satellite, brightness calibration was performed in the laboratory using a source of known brightness such as a quartz iodide bulb and an external filter. The radiometer views the source through the filter and registers "an equivalent brightness compatible with the sun's color temperature" (Conlan, 1973). This sun normalization is dependent upon three angles—the zenith angle of the sun, the scan angle of the satellite, and the angle between the satellite and the sun. However, NESS has used only the correction of the cosine of the solar zenith angle when normalizing the visible data of NOAA 4. Ruff *et al.* (1968) have shown that brightness may vary by a factor of 2 over the range of solar satellite angles. Note that it was not feasible in this study to renormalize the data for the "three angle" geometry.

In addition to the normalization correction, one must relate this correction to the data's location with respect to the earth. Several input parameters are necessary to relate the satellite data to its earth location. These parameters have been thoroughly discussed by Bristor (1970) and are simply listed here. The input parameters are: 1) the orbital elements describing the spacecraft's position; 2) the mounting and alignment of the SR package with respect to the satellite; 3) the angle through which the SR will spin for each earth located sensed target; 4) the location of the horizon for each sweep of the SR; 5) the earth oriented attitude of the spacecraft; and 6) the time relating the SR sweep and the spacecraft's orbital position.

Finally, the scanning radiometer data is mapped in a polar stereographic format. This format can be thought of as a 2048×2048 array whose mesh size is 4 mi near the equator and 8 mi near the pole. The actual mapping and gridding accuracy of the data is, of course, directly related to the accuracy of the input parameters of earth location described above. The primary error source for gridding and mapping of the SR data is the spacecraft attitude error. The spacecraft attitude error is related to the roll/yaw error of the spacecraft.

In addition to attitude error, other gridding error sources include the spacecraft altitude error, satellite positioning error, and the internal satellite time error. The total error involved in mapping and gridding of SR data is normally the sum of the individual error sources; however, based on current use of the satellite product, SR data has a gridding/mapping error of 10 n mi or less (Conlan, 1973).

The scanning radiometer data obtained from NESS was archived on magnetic tape. The digitized data on the tape was in coded values ranging from 0 to 255 for both the infrared and visible channels. The conversion of the coded values for the visual and infrared channels into units of intensity (brightness) and temperature, respectively, are shown in Table 1. A computer program

was written to extract the visual and infrared data from the archive tape. This program was written to take the latitude and longitude of the point of interest from the pilot reports and find the corresponding coded brightness and temperature for that point from the archive tape. However, since there could be mapping and gridding errors of up to 10 n mi inherent to the SR data, it was decided to take an average brightness value around the point of interest to minimize the possible error in the brightness value. To this end, a 5×5 array of brightness points centered around the point of interest was extracted from the archive tape. It was printed and examined to assure that proper extraction was made. A double linear interpolation of the brightness values was then performed with each point weighted by its distance from the center point. The weights used were 10, 20 and 40% (Table 2). Average brightness values for each of the pilot reports selected in Section 2 were obtained.

For example, Table 3 shows the 5×5 brightness array for Eugene, Ore., on 5 May 1975. By multiplying each element in the array in Table 3 by its corresponding element in Table 2 (weight factors) and summing the products, the average brightness of 186.06 is obtained.

When relating the scanning radiometer data to its specific pilot report, the factor of time is important. The scanning radiometer has a fixed pass time, whereas the pilot reports are for many different times. The pilot reports were chosen so that the characteristics of the clouds being reported would not have changed appreciably between the time the PIREP was received and the time of the satellite pass. The maximum time difference between the pass time and PIREPS was 90 min.

4. Three-dimensional nephanalysis data

In order to obtain a second set of independently derived cloud thicknesses and brightnesses data from the 3DNEPH were obtained and are presented here. The 3DNEPH was developed at the Air Force Global Weather Central to incorporate the tremendous quantity of satellite-sensed cloud data and conventionally sensed meteorological parameters into a three-dimensional cloud model of the atmosphere.

Basic to the design of the 3DNEPH is the assumption that satellite information is available for its data in a timely manner. However, in the event that satellite data is not available, the 3DNEPH has the capability of extrapolating past analysis until such time as satellite data does become available.

TABLE 2. Weight factors used for average brightness value.

0.01	0.02	0.04	0.02	0.01
0.02	0.04	0.08	0.04	0.02
0.04	0.08	0.16	0.08	0.04
0.02	0.04	0.08	0.04	0.02
0.01	0.02	0.04	0.02	0.01

TABLE 3. SR data for Eugene, Ore., 5 May 1975.

159	156	186	202	174
159	176	190	196	192
181	164	186	216	194
186	162	183	194	194
192	207	190	189	195

The 3DNEPH program is built as a series of input processors. These processors include the surface data processor, radiosonde observation processor, aircraft data processor, manual data processor, decision tree processor, satellite video data processor, satellite infrared data processor, final processor, forecast processor, verification processor and display processor. Because of the modular nature of the 3DNEPH program, processors can be added to or deleted from the system with a minimum of programming problems. Descriptions and functions of each of the processors can be found in a report by Coburn (1971).

The horizontal resolution of the 3DNEPH program is fixed at 25 n mi. at 60° latitude. This resolution was chosen to facilitate the input of all data types and to provide cloud analyses on a mesoscale grid. The resulting cloud analysis provides a 512×512 array centered at the North (South) Pole of a polar stereographic map. This 512×512 grid was further subdivided into 64 squares (boxes), each containing 4096 grid points to aid in the hemispheric and regional analysis. Once again, each grid point contains information representative of a 25 n mi square centered at the grid point when at 60° latitude. The vertical resolution of the 3DNEPH program divides the atmosphere into 15 layers. The first six layers are terrain following layers and the last nine layers are categorized in feet above mean sea level.

The possible errors inherent to the 3DNEPH with respect to the scope of this study are threefold. First, cloud thicknesses based on surface observation parameters (i.e., height of the cloud base above mean sea level, cloud amount in the base layer and present weather) may be in error since the input for thickness is based on averages and not direct observation. The cloud thicknesses base on infrared satellite data could also be in error since for this study low clouds are exclusively used and the 3DNEPH sometimes interprets low stratus as a clear sky case (Coburn, 1971) because of the relatively small difference in the surface temperature and the cloud radiative temperature. Also, even though the 3DNEPH program makes a correction for atmospheric attenuation in its infrared radiating temperatures, the problem of sensing erroneous cloud top temperatures for layered clouds still remains (Anderson *et al.*, 1971).

Secondly, cloud amounts in different layers, a parameter used to determine cloud thickness, as

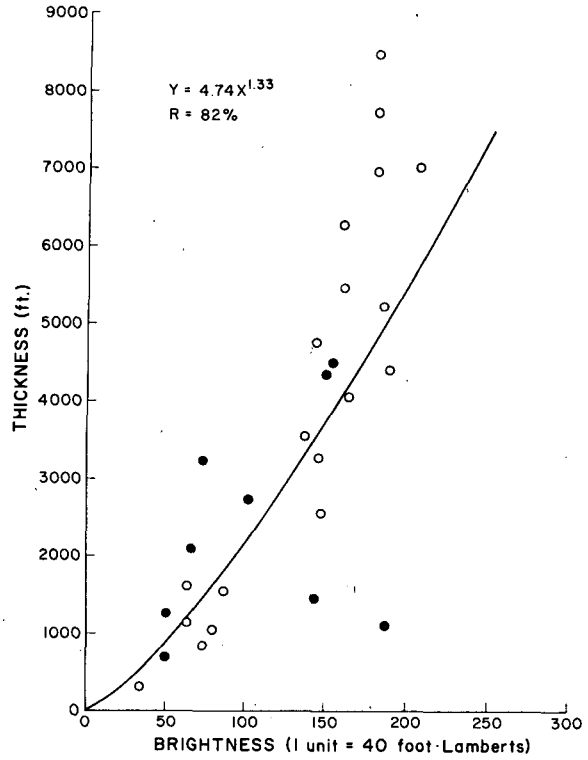

FIG. 4. Regression curve for all pilot report cases. Black dots denote the cases with a maritime tropical air mass origin.

determined by the 3DNEPH's use of aircraft reports would be in error. This is because the 3DNEPH categorizes the aircraft reports into generalized groups [i.e., above clouds (tops less than 10 000 ft.)] and does not use the actual observed cloud-top and/or base measurements of the aircraft reports.

Finally, the third source of error for the 3DNEPH results from the basic assumption that timely satellite data is always available for current analyses. Therefore, the accuracy of the 3DNEPH is a direct result of the availability of timely satellite data.

The 3DNEPH program outputs information concerning each 3DNEPH point and also information for all 15 layers of atmosphere above the point. This information includes cloud types, total coverage of cloud, present weather, maximum top, minimum base, and percent coverage for each of the 15 vertical layers. Three-dimensional nephanalysis data for boxes 43, 44 and 52 (corresponding to the United States) on 4 May 1975 and 10 October 1975 were obtained from the United States Air Force Environmental Technical Application Center at Asheville, N. C.

A computer program was then developed to test each of the 3DNEPH points in these boxes against certain criteria in order to extract cases applicable to this study. The criteria used were that the total coverage be greater than 75%, that no middle or high clouds be present, and that the clouds in the low layers be a continuous deck. After this was accomplished, the output data cases were then screened further to exclude those cases which were over water since information is generally not available other than satellite data. Cases with terrain over 6500 ft were deleted because of the 3DNEPH low cloud parameterization. Scanning radiometer data was then extracted for each of the cases again using a 5×5 array of values around the center point and the weighting scheme used to determine average brightness. The total number of cases were 87.

The time factor was important when relating the scanning radiometer data to the 3DNEPH data. The 3DNEPH data is processed every three hours beginning at 0000Z on a given day. Care was taken to insure that the time of the 3DNEPH data extracted was as close as possible to the scanning radiometer pass time.

There were no DMSP satellite photographs available for 4 May and 10 October 1975, satellite photographs (SMS-2) not shown here were obtained from the National Weather Service for these two days to examine the cloud cover and general cloud conditions.

5. Statistical analysis

a. Description of statistical method

In order to find the statistical relationship between cloud thickness and reflected solar radiance in the visible region of the spectrum (brightness), the data were fitted to a power curve of the form

$$Y=AX^B, \tag{1}$$

where Y=thickness, X=brightness and A and B are the constants to be determined. The least-squares method was employed to arrive at values for A and B in Eq. (1). Then a coefficient of determination R^2 was determined for the data sample. R^2, whose value is between 0 and 1, after being multiplied by 100 is the percent of the variance in the cloud thickness accounted for by the regression curve.

A t test was used to test the coefficient of determination for statistical significance. The t test assumes that the population from which the sample was drawn is from a normal distribution or a near normal distribution. For the coefficient of determination it is defined by

$$t=\frac{R(N-2)^{\frac{1}{2}}}{(1-R^2)^{\frac{1}{2}}}, \tag{2}$$

where R^2 is the coefficient of determination, R is its positive square root, and N is the number of sample points. Therefore, with the assumption of normality, a null hypothesis was formed which stated that the coefficient of determination is equal to zero. A 99.5% confidence level was chosen for the t test with $(N-2)$ degrees of freedom. Therefore, if t [defined in Eq. (2)] is less than or equal to $t_{0.995}$ (a statistical value obtained from a t distribution table of values), the null hypothesis would be accepted, and the conclusion that the coefficient of determination is not significantly different

from zero would be accepted. Consequently, one could conclude that there was little or no correlation between the variables. If t is greater than $t_{0.995}$ then the null hypothesis would be rejected and the conclusion could be drawn that the coefficient of determination was significantly different than zero.

b. Cloud physics parameter

As mentioned in the Introduction, variations in cloud compositions may be an important factor when considering the cloud brightness values. Thus, the air mass concept is used to classify clouds in the statistical analysis. The pilot report cases, excluding those with a maritime tropical air mass origin and their corresponding NOAA 4 cloud brightness values and the 3DNEPH cases, had separate regression analyses performed on them. From a physical point of view one could see how the different air masses would affect the coefficient of determination.

The cloud properties whose characteristics have been measured for different air mass types are droplet concentration and drop size distribution. As described in Fletcher (1969), studies measuring the droplet concentration of the same cloud type in different air masses have been performed. Results for cumulus clouds in maritime and continental air masses showed concentrations of 45 cm^{-3} and 228 cm^{-3}, respectively. Direct

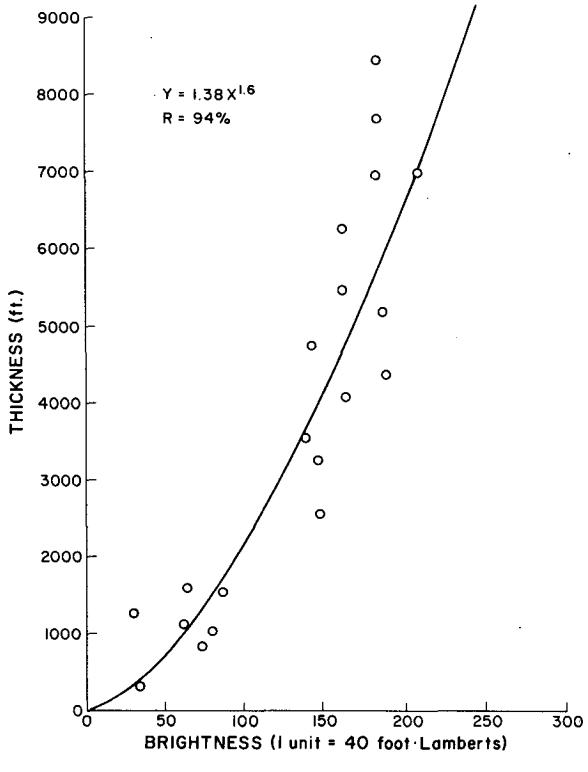

FIG. 5. Regression curve for pilot reports excluding maritime tropical air mass cases.

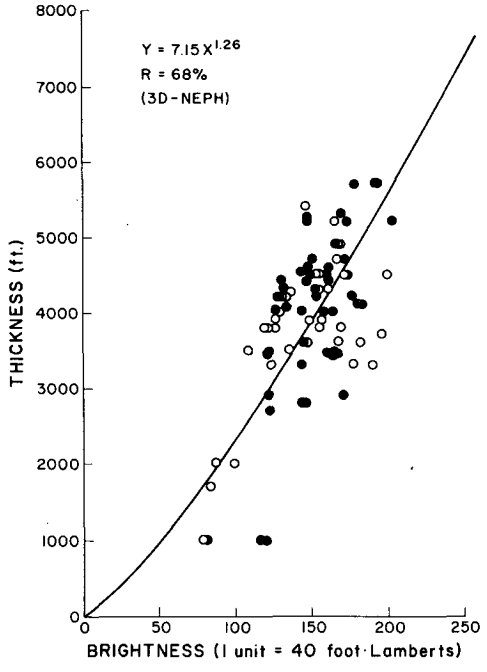

FIG. 6. Regression curve for all 3DNEPH cases. Black dots denote the cases with a maritime tropical air mass origin.

comparisons for layer clouds were not available; however, figures by Squires and Warner (1957) for maritime layer clouds and Diem (1948) for clouds of unknown origin do suggest that differences may be equally as distinct when additional data is collected. For drop size distributions Squires (1958) again has made comparisons of maritime and continental air mass clouds. Maritime cumulus clouds were found to have drop size ranges of approximately 5–55 μm in diameter with an average concentration of approximately 5 cm^{-3}. For continental cumulus clouds the drop size range was approximately 5–15 μm and had an average concentration of approximately 200 cm^{-3}.

The above results show that clouds of maritime origin tend to have smaller droplet concentrations but have many large droplets, and continental air mass clouds tend to have large droplet concentrations of small particles. It is also clear that the droplet size and size distribution within the clouds of maritime origin are being modified constantly through the condensation-collision processes. It is the difference in the droplet size distribution which would affect the reflection and absorption properties of the cloud with respect to incident solar radiation. Therefore, the increase in the coefficient of determination is to be expected when considering solely non-maritime air mass cases, since by excluding these cases some of the variability in the brightness variable is eliminated.

c. Statistical results

For the 28 ($N=28$) thickness and brightness values obtained from the pilot report data, the resultant

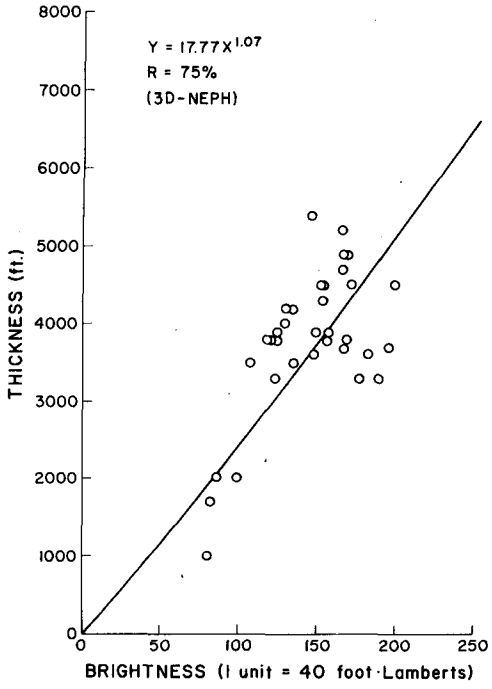

FIG. 7. Regression curve for 3DNEPH excluding maritime tropical air mass cases.

power curve equation (see Fig. 4) was

$$Y=4.74X^{1.33}. \tag{3}$$

The coefficient of determination was 0.66. Using Eq. (2) the value of t was 7.104, and the table value of $t_{0.995}$ with 26 degrees of freedom was 2.779. Consequently, the coefficient of determination, accounting for 66% of the variance in the cloud thickness, is statistically significant. Note that the correlation coefficient R in this case is about 82%.

There were 19 ($N=19$) pilot report cases in nonmaritime tropical air masses. The power curve equation (see Fig. 5) for these brightness and thickness values was

$$Y=1.38X^{1.6}. \tag{4}$$

The coefficient of determination was 0.88 ($R=94\%$). Using Eq. (2), the value of t was 11.166, and the table value of $t_{0.995}$ with 17 degrees of freedom was 2.898. For this data sample the coefficient of determination, accounting for 88% of the variance in the cloud thickness, is therefore statistically significant.

By visual inspection of these two curves (Figs. 4 and 5), it is evident that the variability of the thickness values for a given brightness value in Fig. 4 is drastically reduced by the elimination of the cases in maritime tropical air masses shown in Fig. 5. For example, consider the range of thicknesses corresponding to a brightness value of approximately 190 in Fig. 4. The range is from approximately 1000 to 8400 ft. However, after extracting the maritime tropical cases in Fig. 5, the thickness range for a 190 brightness value is drastically reduced to 4100 ft. Therefore, because the variability in the thickness has been reduced and the R^2 has been increased in Fig. 5, it seems that the rational used in section 5b for excluding the maritime tropical air mass cases is valid.

For the 87 ($N=87$) 3DNEPH data pairs of thickness and brightness, the resultant power curve equation (see Fig. 6) was

$$Y=7.15X^{1.26}. \tag{5}$$

The coefficient of determination was 0.46 ($R=68\%$). Using Eq. (2), the t value was 8.509, and the table value of $t_{0.995}$ with 85 degrees of freedom was 2.646. The coefficient of determination, accounting for 46% of the variance in the cloud thickness, is also obviously statistically significant.

There were 35 ($N=35$) 3DNEPH cases in nonmaritime tropical air masses. The power curve equation (see Fig. 7) was

$$Y=17.77X^{1.07}. \tag{6}$$

The coefficient of determination was 0.55 ($R=75\%$). Using Eq. (2), the t value was 6.351 and the table value of $t_{0.995}$ with 33 degrees of freedom was 2.737. Thus, for this data sample the coefficient of determination, accounting for 55% of the variance in the cloud thickness, is statistically significant.

The 3DNEPH cases were clustered around thicknesses ~3000 to 6000 ft. Few cases were found for thicknesses <3000 ft and no cases were found for thicknesses >6000 ft. Because of this clustering of points and the relative lack of cases at the extremities of the brightness values, the least-squares-regression analysis tended to decrease the exponential nature of the data fit. This is evident from a comparison of the exponents in the regression equations of Figs. 4 and 6. However, even with this clustering of points and the coarseness of the 3DNEPH derived thicknesses (see Section 4) an increase in the R^2 value is still obtained when maritime tropical air mass cases are excluded. Note that one of the reasons for the lower coefficients of determination of the 3DNEPH data as compared to those of the pilot report data is the nature of the 3DNEPH data. As described in Section 4, the thicknesses of the 3DNEPH data are derived from the parameterization of aircraft reports. Thus, the resolution of the 3DNEPH thickness data is coarser than that of the pilot report thicknesses, and as a result larger errors can be introduced.

The data were fitted to other regression curves such as a semilogarithmic curve and a linear curve; however, the best fit obtained, determined by the coefficient of determination, was from the power curve.

6. Conclusions

A direct statistical correlation has been shown to exist between cloud thickness and the reflected solar radiation in the visible part of the spectrum (bright-

ness). Using pilot report derived thicknesses, the regression analysis power curve accounted for more of the variance ($R^2=0.66$) in the observed cloud thicknesses than did a similar regression analysis power curve with 3DNEPH derived thicknesses ($R^2=0.46$).

For both data samples, when a regression analysis was performed using only cases whose origin was not a maritime tropical air mass, the coefficients of determination increased. This shows that brightness values may be used to infer cloud thicknesses more reliably for relatively stable clouds.

Further study in the area of relating cloud thickness and brightness seems to be warranted. Through the use of larger sample sizes containing reliable cloud thickness reports, and further investigation of the physics involved in the interaction of the reflected sunlight and the cloud thickness and composition, a reliable inference of cloud parameters from satellite brightness observations might be obtained. Finally, perhaps the approach of the statistical analysis reported here may also be applicable to multilayered clouds for the inference of their thicknesses.

Acknowledgment. Research work reported in this paper was supported by the Air Force Geophysics Laboratory under Contract F19628-75-C-0107. We thank one of the reviewers for his helpful comments which assisted in the revision.

REFERENCES

Anderson, R. K., and A. H. Smith, 1971: Application of meteorological satellite data in analysis and forecasting. Tech. Rep. AWSTR 212, U. S. Air Weather Service, 223 pp.

Bristor, C. L., 1970: Processing of ITOS scanning radiometer data. *Proc. 1970 Meteor. Tech. Exchange Conf.*, U. S. Air Weather Service, Scott AFB, Ill., 232–242.

Coburn, A. R., 1971: Improved three-dimensional nephanalysis model. Tech. Memo. AFGWCTM 71-2, U. S. Air Force Global Weather Center, 72 pp.

Conlan, E. F., 1973: Operational products from ITOS scanning radiometer data. NOAA Tech. Memo. NESS 52, 57 pp.

Diem, M., 1948: Messungen der Grosse von Wolkenelementen, II. *Meteor. Rundschau*, **9**, 261–273.

Fletcher, N. H., 1969: *The Physics of Rainclouds.* Cambridge University Press, 390 pp. (see pp. 103–121).

Gruber, A., 1975: Comments on "Correlation between cloud thickness and brightness using Nimbus 4 THIR (11.5 channel) and ATS 3 digital data." *J. Appl. Meteor.*, **14**, 643–644.

Liou, K. N., 1975: Can the changes in cloud thickness be monitored from satellite-brightness measurements? *J. Appl. Meteor.*, **14**, 644–645.

——, 1976: On the absorption, reflection and transmission of solar radiation in cloudy atmospheres. *J. Atmos. Sci.*, **33**, 798–805.

Park, S. U., D. N. Sidkar and V. E. Suomi, 1974: Correlation between cloud thickness and brightness using Nimbus 4 THIR data (11.5 channel) and ATS 3 digital data. *J. Appl. Meteor.*, **13**, 402–410.

Ruff, I., R. Koffler, S. Fritz, J. S. Winston and P. K. Rao, 1968: Angular distribution of solar radiation reflected from clouds as determined from TIROS IV radiometer measurements. *J. Atmos. Sci.*, **25**, 323–332.

Schwalb, A., 1972: Modified version of the improved TIROS operational satellite (ITOS D-g). NOAA Tech. Memo. NESS 35, 48 pp.

Squires, P., 1958: The microstructure and colloidal stability of warm clouds, Part I. *Tellus*, **10**, 256–271.

——, and J. Warner, 1957: Some measurements in the orographic cloud of the island of Hawaii and in trade wind cumuli. *Tellus*, **9**, 475–494.

Twomey, S., 1976: Computations of the absorption of solar radiation by clouds. *J. Atmos. Sci.*, **33**, 1087–1091.